

# Green Chemistry

Cutting-edge research for a greener sustainable future

[rsc.li/greenchem](https://rsc.li/greenchem)



ISSN 1463-9262

**TUTORIAL REVIEW**

Chuanling Si, Lin Dai *et al.*

The development of lignin towards a natural and sustainable platform for optical materials



Cite this: *Green Chem.*, 2024, **26**, 9281

## The development of lignin towards a natural and sustainable platform for optical materials

Hai Liu, Yanhua Guan, Li Yan, Yong Zheng, Chuanling Si\* and Lin Dai \*

Lignin is the main component of plant cell walls, conferring upon lignocellulosic biomass both excellent mechanical and barrier properties. At the same time, the considerable number of unsaturated groups and conjugated structures present in lignin render it a promising candidate for applications in the optical domain. In recent years, the development of the optical properties of lignin and lignin-derived optical materials has paved the way for a novel avenue of lignin valorization. This review is concerned with the mechanisms of lignin-derived optical materials, with particular emphasis on the physical and chemical structures that are linked to their optical performance, including UV absorption, photothermal conversion, and photoluminescence. Additionally, the potential applications of these materials in energy storage, bio-imaging, structural materials, and photonic crystal are also presented, demonstrating the unique optical properties of lignin. Finally, the challenges and future directions of lignin as an optical material are presented, with the objective of developing lignin into a polymer biobased raw material that can serve advanced emerging industries.

Received 18th June 2024,  
Accepted 24th July 2024

DOI: 10.1039/d4gc02944e

rsc.li/greenchem

### 1. Introduction

In the vast and intricate natural world, lignin is akin to a magical light-manipulating wizard that absorbs and scatters

ultraviolet light, thus providing plants with natural UV protection and improving their survival and adaptability.<sup>1,2</sup> The study of the optical properties of lignin, derived from the natural properties of lignin, has become an important direction for the development of new materials. The lignin utilized in current research is derived from industrial sources, specifically from byproducts of the pulp and biorefinery industries.<sup>3</sup> Notably, the color of lignin undergoes a notable change from colorless to brownish-black during the extraction process.<sup>4</sup> This interesting optical phenomenon has attracted the attention of researchers.<sup>5-7</sup> In light of the accelerated advancement of chemical theory and biological technology, the underlying principle of light manipulation is gradually being revealed to reside in its physical and chemical structures.<sup>8,9</sup>

Lignin is a natural polymer that possesses a large number of unsaturated groups and conjugated structures. These properties enable it to exhibit optical phenomena such as light absorption,<sup>10</sup> emission,<sup>11</sup> and fluorescence.<sup>12,13</sup> Currently, lignin is mainly obtained through industrial processes such as pulping and biorefining. Following the application of acids, alkalis, high temperatures, and other disruptive separation techniques, natural lignin undergoes degradation and condensation, resulting in the formation of a multitude of chromophores (carbon-carbon double bond conjugated aromatic rings and quinone methyl and quinone groups) and homochromatic groups (phenolic hydroxyl groups).<sup>14</sup> Despite the darker coloration of technical lignins, they also present a greater range of possibilities for their optical properties. Nevertheless, lignin is extracted by a multitude of methods,

State Key Laboratory of Biobased Fiber Manufacturing Technology, Tianjin Key Laboratory of Pulp and Paper, Tianjin University of Science and Technology, Tianjin 300457, China. E-mail: sichli@tust.edu.cn, dailin@tust.edu.cn



Lin Dai

*Dr Lin Dai is currently a professor at Tianjin University of Science and Technology. He obtained his PhD in Chemical Engineering (Forestry Products) from Beijing Forestry University, China. In 2016, he joined the faculty of Tianjin University of Science and Technology. His research interests are focused on the development of lignin with particular functions and various forms, including nanoparticles, hydrogels, and polymer compo-*

*sites. To date, he has authored and co-authored more than 100 journal papers with an H-index of 42. Dr Dai's contributions have been recognized with the Liang Xi Award for Progress in Science and Technology.*

which results in a diverse range of structural compositions and a lack of stability in performance, thereby hindering the standardization and high-value applications of technical lignin. The inherent potential of technical lignin can be unleashed through physical and chemical structure modulation, thus promoting its application in the production of photothermal, photovoltaic, and bio-optical materials, and other high-value-added products.<sup>15–28</sup> Kraft lignin, in particular Indulin kraft lignin, is distinguished by its high concentration of guaiacyl units. The methoxy and phenolic groups present in the guaiacyl units serve to enhance the ability of the latter to absorb UV light. Soda P1000 lignin contains a substantial proportion of *p*-coumarate units. The conjugated double bonds and phenolic structures present in the *p*-coumarate units facilitate enhanced absorption of UV light and emission of visible light, thereby augmenting the fluorescence properties of the material. Alcell lignin, produced at a pilot plant scale without the addition of a catalyst, exhibits a notable degree of condensation.<sup>29</sup> The elevated condensation level increases the rigidity of the lignin polymer, thereby enhancing its stability under UV excitation and reducing non-radiative decay rates, which may potentially result in an elevated fluorescence quantum yield.<sup>30</sup> Compared with conventional optical materials, lignin embodies good environmental friendliness and sustainability due to its unique aromatic structure and renewability, thus highlighting its competitiveness in the development of green optical materials.

In recent years, lignin has undergone rapid development in terms of its physicochemical structures, with the acquisition, transformation, and utilization of sunlight, laying a solid foundation for the study of lignin as an optical material. In terms of application, the potential of lignin in the field of optical materials has become increasingly apparent with the in-depth study of its optical properties. Lignin exhibits excellent light absorption and fluorescence properties, as well as realizes the tunability of light emission through structural modulation, which makes it show broad application prospects in the fields of solar cells, optical sensors, and fluorescent markers. This review provides a comprehensive overview of the properties and applications of lignin and its composites as natural, sustainable optical materials. In this review, we highlight the relationship between the lignin structure and optical properties, including an exploration of the fundamentals of UV absorption, photothermal conversion, and photoluminescence characteristics. The relationship between the molecular structure and optical properties of lignin is analyzed in depth, which is crucial for its application as an optical material. Furthermore, in light of recent advances in lignin in the optical field, we provide a comprehensive summary of the applications of high-performance sustainable lignin-derived materials, including materials such as photothermal, photoelectric, and organic fluorescent materials, providing pathways for lignin valorization (Fig. 1). Finally, we delve into the challenges and future directions for lignin as an optical material, enabling this natural “wizard” to shine anew in modern technology.

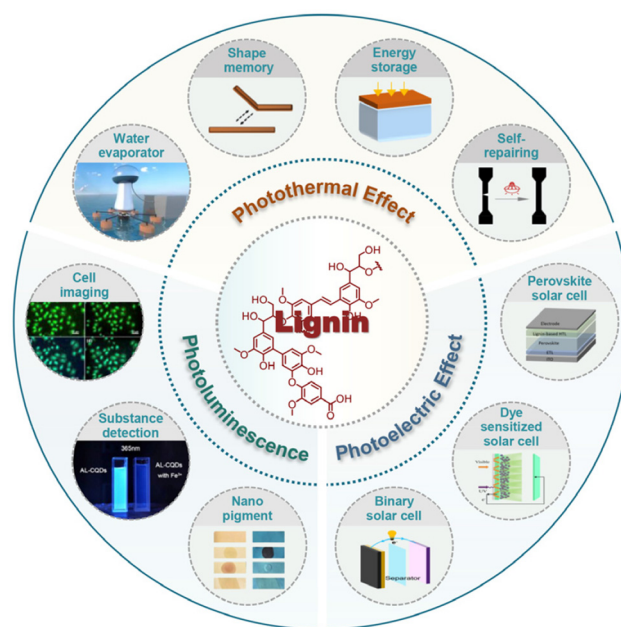


Fig. 1 Optical properties of lignin and its application in the field of functional materials.

## 2. Optical properties of lignin

In order to gain a comprehensive understanding of the structure and function of lignin, researchers have conducted a large number of detailed structural characterization studies of lignin. Many remarkable features of the structure, composition and chemical bonding of lignin have been revealed by solution and solid-state NMR,<sup>32</sup> gas chromatography,<sup>33</sup> liquid chromatography,<sup>34</sup> UV-visible absorption spectroscopy,<sup>35</sup> Fourier transform infrared spectroscopy,<sup>36</sup> Raman spectroscopy,<sup>37</sup> scanning electron microscopy/transmission electron microscopy,<sup>38</sup> and other techniques. In addition, the low conjugated structures of lignin have relatively few double bonds and a close arrangement of aromatic rings. Medium-conjugated lignins exhibit intermediate levels of aromatic ring linkages and  $\pi$ -electron delocalization, which enhances their absorption of UV and visible light while also enhancing their emission and fluorescence properties. Strongly conjugated lignin structures are distinguished by extensive  $\pi$ -electron delocalization between multiple aromatic rings, and the extensive conjugation leads to significant light absorption, strong fluorescence, and enhanced photoprotective properties (Fig. 2).<sup>31</sup>

### 2.1. Ultraviolet absorption

Lignin, as a natural aromatic polymer, contains a large number of benzene rings, double bonds and carbonyl structures in its macromolecular structure, which gives lignin good UV-absorbing properties.<sup>39–41</sup> These properties are mainly attributed to the abundance of functional groups in lignin, including phenolic, ketone, and quinone structures and other chromophores.<sup>40,42–44</sup> Some common chromophores found in

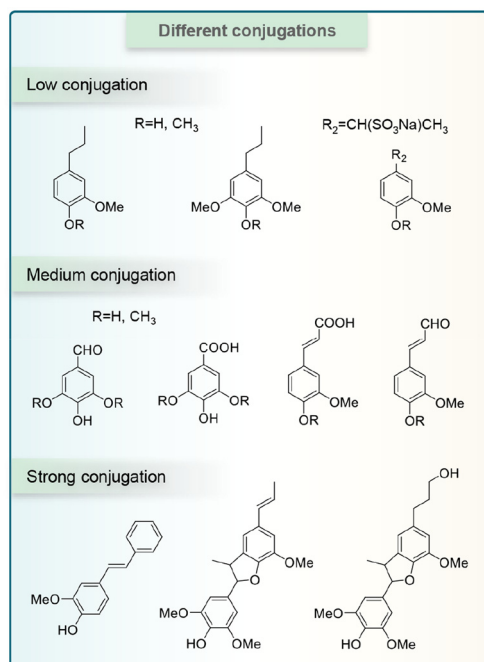


Fig. 2 Schematic diagram of several typical modes of conjugation within the lignin molecule.<sup>31</sup>

lignin are shown in Fig. 3A.<sup>45</sup> Previous studies have shown that free and etherified phenolic hydroxyl groups in the lignin structure exhibit absorption near 280–290 nm, while double bonds and/or carbonyl groups conjugated to phenyl groups exhibit absorption between 300–400 nm.<sup>46,47</sup> Ultraviolet light entering the surface of the Earth is composed primarily of UVA (320–400 nm) and a minor component of UVB (290–320 nm).<sup>48</sup> Therefore, the UV resistance of lignin may be significantly influenced by the double bond and/or the linkage structure formed by the carbonyl group and the phenyl group. In addition, it has been reported that the syringyl (S) phenolic group contains a greater quantity of functional methoxy than the guaiacyl (G) and *para*-hydroxyphenyl (H) phenolic groups. It has been established that lignified plants are protected against both microbial attack and damage by UV radiation. It can be concluded that plants with a higher lignin content exhibit superior UV resistance.<sup>49</sup> Consequently, lignin has been widely used in the manufacture of UV-protective materials.<sup>50–52</sup>

## 2.2. Photothermal

Photothermal conversion materials are capable of effectively converting light energy into heat energy, representing an

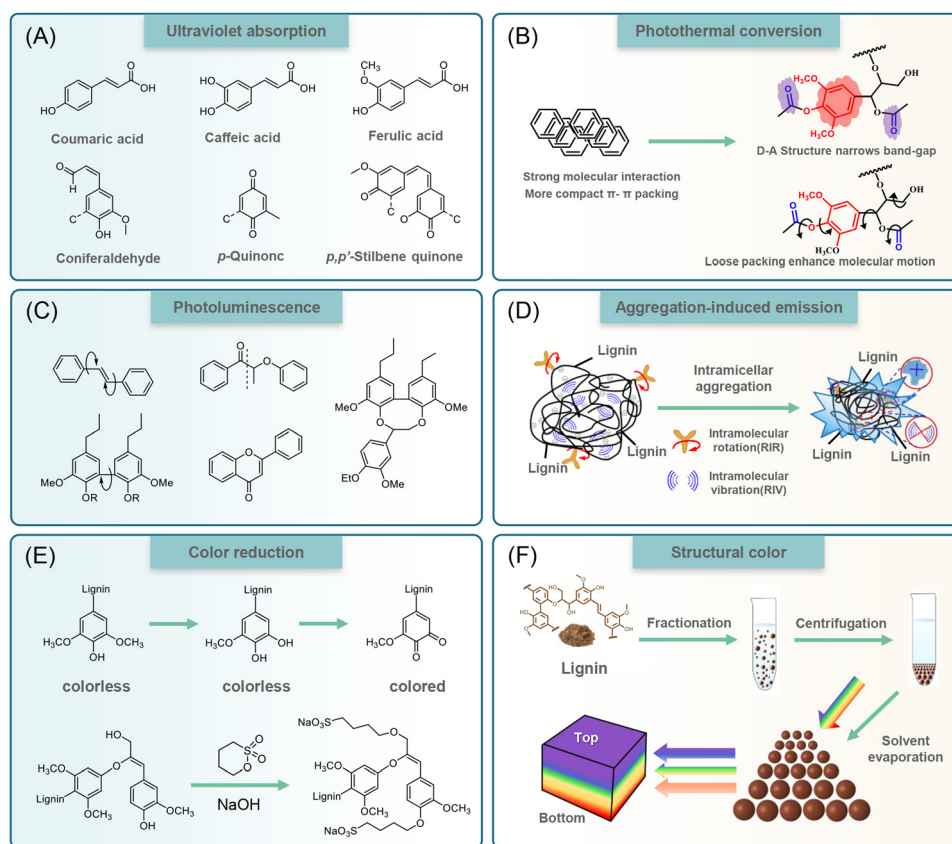


Fig. 3 Linkage between the structure of lignin and its optical properties. (A) Schematic of common chromophores in lignin.<sup>45</sup> (B) Schematic representation of the mechanism for enhancing the photothermal effect of acetylated lignin.<sup>60</sup> (C) Schematic representation of model compounds with large effects on lignin fluorescence.<sup>61–66</sup> (D) Schematic representation of the intramolecular aggregation-enhanced emission of lignin.<sup>67</sup> (E) Schematic diagram of the lignin color generation mechanism and the color reduction mechanism.<sup>68</sup> (F) Schematic representation of the preparation of photonic crystals from lignin.<sup>69</sup>

effective approach for utilizing light energy. Common photo-thermal materials, including graphene,<sup>53,54</sup> carbon nanotubes,<sup>55,56</sup> and carbon quantum dots,<sup>57,58</sup> have been widely used in photothermal conversion systems.<sup>59</sup> Organic conjugated materials have several advantages, including high tunability in design, light weight, flexibility, and malleability. Lignin is a complex aromatic biopolymer with a large number of aromatic rings and conjugated functional groups in its molecular structure. These conjugated structures can effectively promote the electron transition from low-energy orbitals to high-energy states and release energy through non-radiative leaps, thus achieving efficient photothermal conversion.<sup>70–74</sup> The  $\pi$ - $\pi$  conjugated stacking and strong intermolecular interactions play a pivotal role in the photo-thermal conversion of lignin. Upon photoexcitation, the  $\pi$ - $\pi$  conjugated structure of lignin facilitates the electron jump from the ground state to the excited state. The excited state electrons are released in a nonradiative form when they jump back to the ground state, resulting in a high photo-thermal conversion efficiency. Lei *et al.* proposed a mechanism by which the electron-absorbing groups enhance the photo-thermal effect of lignin. This mechanism involves the introduction of electron-absorbing groups such as acetyl, which constructs electron donor-acceptor structures in the lignin molecule, leading to the narrowing of the band gap and the enhancement of the light absorption of acetylated lignin. The reduction of the acetylated lignin results in the reduction of hydrogen bonding, the weakening of intermolecular interactions, and the enhancement of molecular motions, which promotes non-radiative attenuation and ultimately improves the efficiency of photothermal conversion (Fig. 3B).<sup>60</sup>

### 2.3. Photoluminescence

Photoluminescence is the process of light energy absorption, energy transfer, and emission. When ultraviolet, infrared, or near-infrared light strikes lignin, electrons in the lignin molecule are excited. Upon returning to the ground state, these electrons release energy in the form of photons. Researchers employed a model object study to investigate lignin fluorophores by comparing the fluorescence properties of model objects with a single benzene ring and multiple conjugated structures. Lang *et al.* conducted a study on the aggregation-induced luminescence effects of phenylacrylic acid and stilbene-based modelers.<sup>61</sup> Castellan *et al.* examined the fluorescence properties of the modelers in solid films and discovered that the fluorescence emission wavelengths of these modelers were longer in the solid state than in the solution state.<sup>62</sup> Tylli *et al.* identified fluorophores by linear weighted fitting.<sup>63</sup> Albinsson *et al.* investigated the effect of *cis-trans* isomerization on the fluorescence. The *trans* structure exhibited strong fluorescence, whereas the *cis* structure did not show any fluorescence at room temperature.<sup>12</sup> Additionally, Gardrat *et al.* explored the effect of etherification of phenolic hydroxyl on the fluorescence. The replacement of the phenolic hydroxyl with methyl or phenylmethyl substituents resulted in a significant decrease in fluorescence quantum efficiency.<sup>64</sup> Lähdeci

*et al.* found that the conjugated 5–5 bond had significant fluorescence emission.<sup>65</sup> Radotić *et al.* analyzed the fluorescence spectra of dehydrogenated oligomers of coniferyl alcohols by using the reverse convolution technique (Fig. 3C).<sup>66</sup> These studies advance the understanding of the fluorescence properties of lignin.

### 2.4. Aggregation-induced emission

In recent years, novel luminescent materials with aggregation-induced/enhanced emission properties have received increasing attention due to their potential applications in the fields of optoelectronic materials, chemical sensors and biomedical probes.<sup>75,76</sup> Aggregation-induced luminescence is a phenomenon whereby a specific molecule exhibits low or no fluorescence when in a monomeric form, but its fluorescence properties are significantly enhanced when forming aggregates.<sup>77</sup> Xue *et al.* demonstrated that the aggregation state of lignin could be controlled by increasing the proportion of non-good solvents in mixed solvents, and that the intensity of fluorescence emission increased significantly upon aggregation enhancement. In addition, electrostatic interaction studies showed that sulfonated alkaline lignin exhibited a comparable fluorescence enhancement effect in the presence of cetyltrimethylammonium bromide, whereas alkaline lignin showed aggregation fluorescence quenching (Fig. 3D).<sup>67</sup> Yan *et al.* investigated the concentration-dependent aggregation behaviors of lignin sulfonate and alkaline lignin, respectively, and found that the aggregation resulted in a red-shift. The fluorescence excitation spectra exhibited a shift due to the J-aggregation effect,<sup>78–80</sup> which was further verified by Ma *et al.*<sup>81</sup> Overall, the aggregation behavior of lignin significantly affects its fluorescence properties, and the aggregation-induced luminescence and J-aggregation behaviors play a key role in the fluorescence enhancement.<sup>67</sup> These findings contribute to the in-depth understanding and application of the fluorescence properties of lignin.

### 2.5. Color reduction

Lignin is nearly colorless in wood, but alkaline lignin that is separated from pulping black liquor has a strong black color.<sup>4</sup> Of all the lignin color-generating or color-enhancing groups, the quinone-type structure produces the most severe effects.<sup>82</sup> As illustrated in Fig. 3E, lignin contains methoxyl groups, which are readily converted into phenolic hydroxyl groups during pulping or other lignin separation processes. These hydroxyl groups are subsequently transformed into quinone-type structures, ultimately leading to the darker color expression of technical lignin. It has been demonstrated that the color change of lignin can be slowed down by sulfonation with hydroxyl group closure, because the closure of hydroxyl groups prevents the transformation of the phenolic hydroxyl groups into the quinone-type structure.<sup>68</sup> The color-reducing modification of technical lignin can facilitate the expansion of the application areas and significantly enhance its utilization value. Alkaline H<sub>2</sub>O<sub>2</sub> treatment removes or leads to selective reaction with the chromophore structure while retaining the

lignin native structure.<sup>83</sup> The combination of H<sub>2</sub>O<sub>2</sub> and UV light also removes the chromophores. The application of H<sub>2</sub>O<sub>2</sub> to the wood surface and subsequent irradiation with UV light to remove the light-absorbing chromophores lead to a reduction in the use of chemicals.<sup>84</sup> In addition, the formation of nanoparticles with a uniform spherical shape, in which hydrophobic chromophores are located in the inner core, has been observed in lignin modified by organic isocyanate in an ethanol–water mixed solvent system. During solvent-controlled encapsulation, the organic isocyanate and hydroxyl groups reacted during solvent-controlled encapsulation, contributing to the decolorization of the lignin derivatives by converting the phenolic hydroxyl groups to quinone structures.<sup>85</sup>

## 2.6. Structure color

Many colors in nature are not formed directly from pigments, but originate from the scattering and diffraction of light by specific material structures.<sup>86,87</sup> In recent studies, the application of lignin colloidal spheres provides a sustainable and biocompatible way to mimic this natural phenomenon. By precisely controlling the self-assembly of these monodisperse particles from lignin, ordered microstructures can be formed, which in turn produce rich color effects. Wang *et al.* prepared monodisperse lignin colloidal spheres by a solvent/nonsolvent self-assembly method, and the structural color could be tuned by precisely controlling the sphere size.<sup>88</sup> Liu *et al.* investigated the importance of the centrifugation process for the size classification of lignin nanoparticles and its effect on the photonic crystal structure. The centrifugation process enables the short-range ordering of lignin colloidal spheres in solution to form photonic crystals by adjusting the speed and time for effective particle size classification based on the hydrodynamic diameters of the lignin nanoparticles. The ordered structure is essential for realizing and regulating the structural color (Fig. 3F).<sup>69</sup> The development of lignin-based structural colors is still in its early stages and further understanding of their formation and properties is essential. This progress represents a significant step forward in paving the way for value-added lignin-derived optical materials.

## 3. Application of lignin-derived optical materials

### 3.1. Energy storage materials

Lignin absorbs light *via* its aromatic rings, converting it into chemical energy. This process is crucial for phototransduction, photo-sensing, and photoprotection. At the molecular and micro-nano scales, lignin's photostorage efficiency is enhanced by its nanoscale structure, functional groups, and interactions with other materials. These properties make lignin a promising material for sustainable photostorage applications such as photothermal and photoelectric conversion.

**Photothermal materials.** Photothermal materials provide an efficient means of directly utilizing solar energy. In this context, lignin, as a photothermal material, exhibits strong

light absorption capabilities, excellent thermal conductivity, and remarkable flexibility and adaptability. Consequently, it has a wide range of applications in areas such as self-repairing, shape memory, energy storage and solar steam power generation (Fig. 4A). Yang demonstrated a sustainable porous scaffold consisting of periodate oxidized wood (POW) as a support material with *in situ* retained lignin as a light-absorbing dopant. The stacking ability of the lignin molecules gives the materials enhanced light absorption, high photothermal conversion efficiency (~86.7%) and high latent heat (151 J g<sup>-1</sup>) for higher maximum energy storage.<sup>91</sup> However, the photothermal conversion efficiency of primitive lignin is limited, and the interfacial heat conduction between lignin and polymers is weak. Furthermore, the lack of an efficient thermal energy conversion management system during the photothermal conversion process results in a large amount of heat dissipation and heat loss.<sup>92</sup> To address this issue, Tu *et al.* proposed a ligand-assisted sunflower photothermal conversion technology, which utilizes polyethylene propylene diene monomer rubber and lignin as the photothermal conversion medium. This approach involves the optimization of photothermal conversion, interfacial heat transfer and a macroscopic photothermal driving process through ligand bonding. The lignin-containing material exhibits rapid light-induced heating, reaching a temperature of 180 °C in 20 s and then gradually stabilizing at 199 °C through the coordination of Zn<sup>2+</sup> (Fig. 4B).<sup>70</sup> Zhou *et al.* reported a demethylation method to increase the photothermal conversion temperature of lignin for solar-driven atmospheric water harvesting. The surface temperature of demethylated lignin reached 67.2 °C after 10 min of exposure to standard sunlight. This high photothermal performance is mainly attributed to the increased phenolic hydroxyl content, which enhances the  $\pi$ - $\pi$  conjugated structure of the lignin aromatic ring.<sup>93</sup> Yang *et al.* synthesised a lignin with a high polyphenolic hydroxyl content through phenolic modification and prepared a polyphenolic lignin-based vitrimer. The surface temperature of this vitrimer can reach 229 °C in 25 s under 808 nm infrared light irradiation at 1.00 W cm<sup>-2</sup>. Based on this performance, the lignin-based vitrimer can be recycled and remodelled under infrared light irradiation.<sup>94</sup> Li employed the conjugated structure in lignin to facilitate the electron jump from low-energy orbitals to high-energy states, thereby enabling the preparation of smart elastomer composites with diverse functionalities. These composites exhibit a good light-triggered shape memory effect and excellent light-controlled self-repair performance (up to 98.2% efficiency) (Fig. 4C).<sup>71</sup> Jin *et al.* prepared enzymatically hydrolyzed lignin-derived shape memory polymers by taking advantage of the rigid benzene ring structure and excellent photothermal properties of lignin. When subjected to simulated solar irradiation (2000 W m<sup>-2</sup>), enzymatically hydrolyzed lignin-derived shape memory polymers with a lignin content of 50 wt% exhibited surface temperatures as high as 105 °C and achieved shape memory within 20 s (Fig. 4D).<sup>89</sup>

Seawater desalination technology has garnered widespread attention.<sup>95-97</sup> Lignin has emerged as an optimal substrate

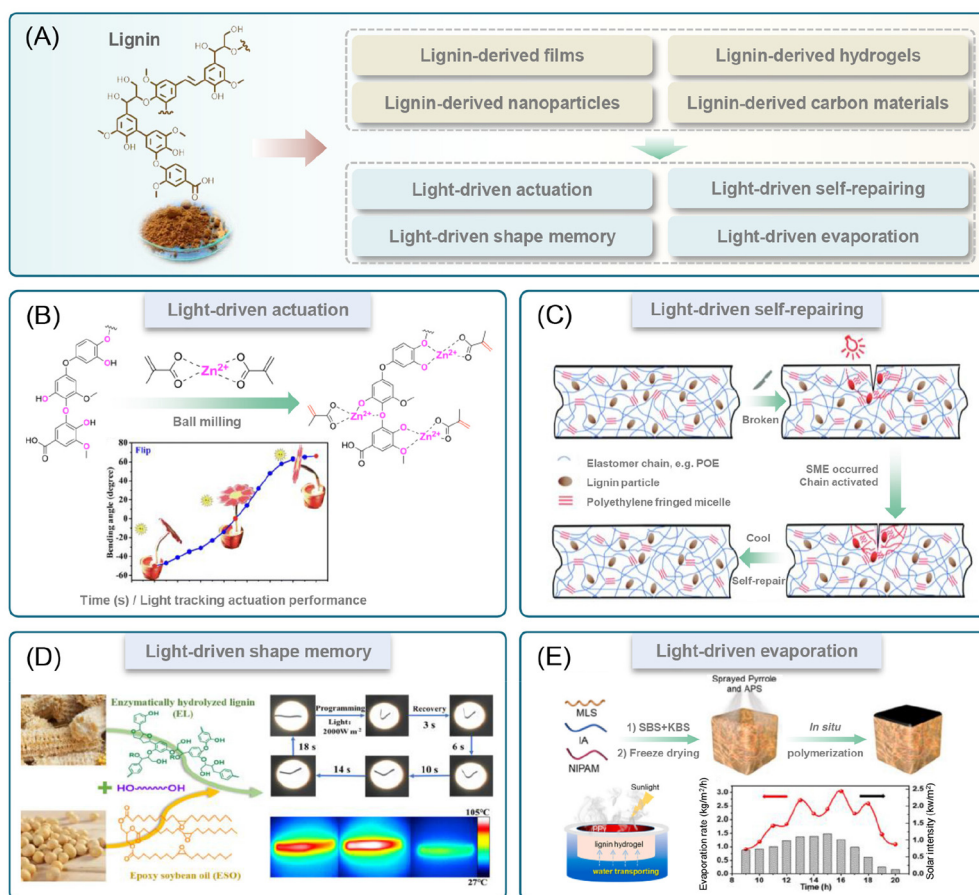


**Fig. 4** Multifunctional applications of lignin in light-to-heat conversion. (A) Schematic diagram of various lignin-based forms in light-to-heat applications. (B) Schematic of the preparation process of a lignin-based composite photoconductive material and its fast-tracking light performance.<sup>70</sup> (C) Schematic diagram of the self-repairing mechanism of lignin/elastomer composites based on the lignin photothermal effect.<sup>71</sup> (D) Schematic diagram of enzymatically hydrolyzed lignin-based light-driven shape memory polymers.<sup>89</sup> (E) Digital images of the lignin hydrogel-based evaporator samples.<sup>90</sup>

material for solar interfacial evaporation systems due to its porosity, hydrophilicity, high strength-to-weight ratio, and thermal insulation properties. Jeon *et al.* employed lignin nanoparticles and cellulose nanofibers as bio-renewable photoabsorbents and hydrophilic carriers, respectively, to develop a highly efficient interfacial heating system.<sup>98</sup> Jiang *et al.* prepared a lignin-based hydrogel with a three-dimensional mesoporous/microporous structure. The developed lignin-based hydrogel evaporator demonstrated the ability to operate continuously for 24 h with a stable evaporation rate of 2.25 kg m<sup>-2</sup> h<sup>-1</sup> and good stability within the pH range of 1–14 (Fig. 4E).<sup>90</sup> Chen *et al.* used liginosulfonate as a raw material to prepare a liginosulfonate-based carbon material (CLS) through carbonization. Concurrently, they prepared liginosulfonate-based porous charcoal (PCLS) with calcium carbonate as an activator. The two types of charcoal powders were then utilized as light absorbers and crosslinked with poly(vinyl alcohol) to create solar energy interfacial evaporation materials (PVA@PCLS and PVA@CLS), exhibiting a significant increase under 1 kW m<sup>-2</sup> irradiation.<sup>99</sup> Similarly, Lin *et al.* constructed

an all-lignocellulose-based bilayer hydrogel using a cellulose–lignin composite hydrogel as the substrate and lignin-derived carbon as the photothermal material. The presence of lignin increases the hydrophilicity of the hydrogel and maintains the capillary channels of the hydrogel, which transforms water into an intermediate state and reduces the enthalpy of evaporation of water.<sup>100</sup> Recently, another research team fabricated a lignin/wood-based solar evaporator using a salt-resistant, all-wood material that can be used for a long period of time. The lignin in the evaporator serves not only as a photothermal material for converting light energy into heat, but also enhances the structural strength of the evaporator. Furthermore, the photothermal conversion capacity is up to 91.74%.<sup>101</sup> Lignin-based solar interfacial evaporators offer the advantages of low production cost, low energy consumption, and low pollution, providing a promising solution to the environmental problem of freshwater depletion.

**Photoelectric materials.** In recent years, numerous studies have been conducted with the objective of developing and implementing lignin photoelectric conversion technologies.

To date, there are many ways of preparing lignin-based photoelectric conversion materials including a 3D thermally conductive pathway,<sup>91</sup> surface carbonization, overall carbonization, structural design, and surface coating with photothermal materials.<sup>102–104</sup> These methods have been shown to effectively utilize natural light energy and have the potential to be applied to solar cells, photoelectric sensors and other fields. As a cutting-edge renewable energy technology, solar cells have the potential to revolutionize the energy industry. Their high conversion efficiency, stability, and cost-effectiveness are key factors that make them a promising candidate for industrialization.

The hole transport layer (HTL) plays a pivotal role in the functioning of solar cells. It was found that lignin-containing phenol structural units with hole-transport properties could be used as a conjugated conventional polymer.<sup>105</sup> Wu *et al.* grafted sulfonated acetone–formaldehyde onto alkaline lignin, and prepared grafted sulfonated acetone–formaldehyde lignin (GSL) by reaction, dialysis and drying to form water-dispersed PEDOT:GSL. The short-circuit current density, fill factor and open-circuit voltage enhancement of high-performance perovskite solar cells were enhanced by the use of PEDOT:GSL as a hole extract layer, resulting in an increased power conversion efficiency from 12.6% to 14.94%.<sup>102</sup> In carbon-based battery materials, lignin differs from graphite in that the polymeric nature of lignin allows for functionally tailored modifications, resulting in carbon materials with a variety of morphologies and enhanced functional properties. This enables lignin derivatives to exhibit beneficial properties throughout the chain of the battery component development process. Consequently, lignin is highly structurally flexible and multi-

functional, rendering it an attractive precursor material for carbon-based battery materials.<sup>106</sup>

The demand for low-temperature, solution-processable HTLs for solar cells has led to the use of polyaniline as an alternative HTL for a variety of electronic devices, but conventional polyaniline is limited by its processability and can be insoluble in common organic solvents. In contrast, lignin as an HTL has better processability and conductivity, which can effectively make up for the lack of polyaniline in solar cells. Al-Dainy *et al.* prepared a conductive polymer comprising ligno-sulfonic acid grafted polyaniline doped camphor sulfonic acid and applied it as an HTL to doped hydride solar cells. This process resulted in optimized solar cell performance, as evidenced by the tuning of the morphology and performance metrics of the lignosulfonic acid grafted polyaniline doped camphor sulfonic acid films. The films exhibit high crystallinity and large grain sizes (>5  $\mu\text{m}$ ), which effectively reduce the number of intergranular boundaries, in turn decreasing the rate of electron and hole complexation in the chalcogenide layer and increasing the charge extraction efficiency and transport rate.<sup>107</sup> Li *et al.* developed a PEDOT/lignosulfonate cross-linked composite film directly using lignosulfonate, which exhibits the features of large functionality, good uniformity, and excellent water resistance, and a power conversion efficiency of 12.9%, which is comparable to that of PEDOT/PSS. Cells made of PEDOT:lignosulfonate films demonstrate enhanced durability in  $\text{N}_2$  and air under non-encapsulated conditions (Fig. 5A).<sup>108</sup> Hu *et al.* successfully prepared an efficient isotropic electron transport interfacial layer based on demethylsulfated lignin ( $\text{D}_{\text{Me}}\text{KL}$ ) and perylenediimide (PDIN). This transport interfacial layer exploits both the special three-

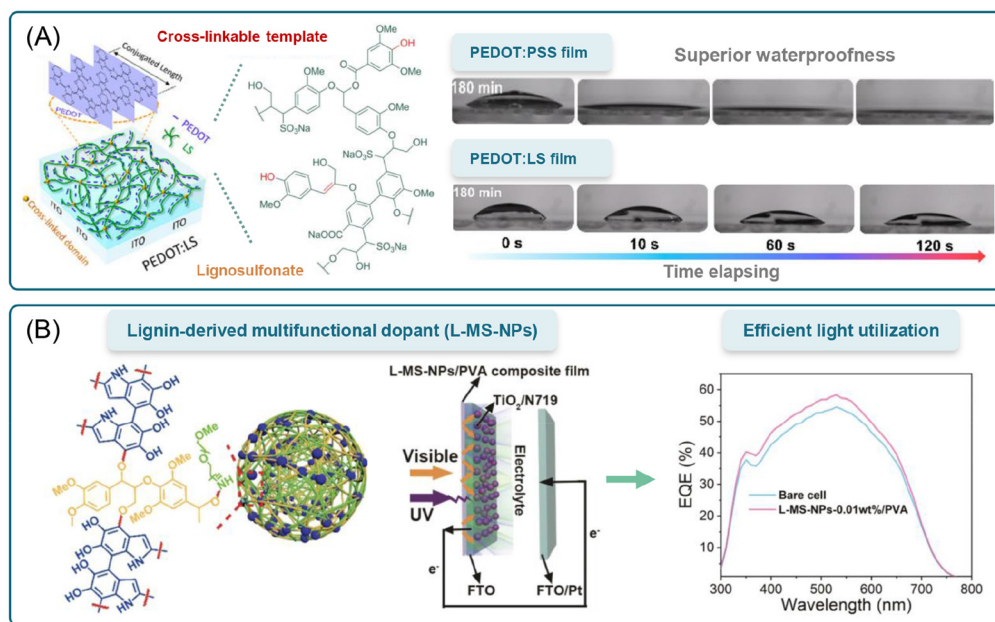


Fig. 5 (A) Schematic diagram of the structure of PEDOT:LS and its superior waterproofness in PSC.<sup>108</sup> (B) Schematic diagram of L-MS-NPs applied to photoluminescent and haze films in DSSCs.<sup>109</sup>

**Table 1** Lignin modifications for use in phenolic resin

Types	Applications	Type	Efficiency	Ref.
Alkaline lignin	Hole transport layer	PSC <sup>c</sup>	14.94%	102
Lignosulfonate	Hole transport layer	PSC	10.8%	107
Lignosulfonate	Hole transport layer	PSC	12.85%	108
Kraft lignin <sup>a</sup>	Electron transport layer	OSC <sup>d</sup>	16.02%	110
Kraft lignin	Cathode interface layer	OSC	15.73%	117
Lignin <sup>b</sup>	Counter electrodes	DSSC <sup>e</sup>	9.22%	118
Enzyme lignin	Photoluminescent and haze films	DSSC	4.1%	109

<sup>a</sup> Demethylated kraft lignin. <sup>b</sup> Oxygen–nitrogen–sulfur codoped lignin. <sup>c</sup> PSC represents perovskite solar cells. <sup>d</sup> OSC represents organic solar cells. <sup>e</sup> DSSC represents dye-sensitized solar cells.

dimensional mesh structure of D<sub>Me</sub>KL and the high electrical conductivity of PDIN, which significantly improves the electron transfer and collection in both the cross-section and the vertical cross-section, resulting in an optimal power conversion efficiency of 16.0% for the organic solar cell with the D<sub>Me</sub>KL/PDIN interlayer (Table 1). This is higher than that of the pristine PDIN interlayer (15.4%). In addition, the phase separation issue can be solved due to the interaction of the D<sub>Me</sub>KL and PDIN chemical bonds.<sup>110</sup>

Interfacial engineering represents a crucial tool for the development of highly stable and cost-effective solar cells, which is due to the necessity of maintaining chemical inertness between the thick ring electron acceptor and the cathode interfacial layer in solar cells.<sup>111–116</sup> In addition to its capacity to synthesize HTL materials, lignin can also demonstrate its superior performance in optimizing the interfacial properties of solar cells. Zhang *et al.* successfully achieved work function modulation at the cathode interface in solar cells using a strategy of binary interfacial materials based on lignin. They also characterized lignin-derived organic photovoltaic cells in terms of device performance and stability mechanism. The combination of kraft lignin and bathocuproine significantly enhanced organic solar cell stability, benefiting from electron transfer and hydrogen bonding between the phenol groups and the phenanthroline on the lignin. This enables the binary interfacial layer to achieve work function modulation, allowing it to adapt to different active components, which is a significant advance in organic solar cells that effectively use bio-based materials. The introduction of lignin not only blocks the substantial contact between bathophenanthroline and the non-fullerene material on a spatial scale, but also attenuates the electron-rich nature of bathophenanthroline from a chemical perspective. Consequently, the lignin-based binary interface strategy can effectively inhibit its chemistry and improve the efficiency and stability of the device.<sup>117</sup> Replacing activated carbon in supercapacitors with lignin not only improves performance but also reduces costs. The use of 3D polymers of lignin enables the formation of hydrogels and aerogels, which can be combined with pseudocapacitive materials and spun into individual flexible fiber electrodes.<sup>119–121</sup>

Carbon materials represent a promising avenue for the development of effective counter electrodes in dye-sensitized

solar cells (DSSCs). However, many of these materials, including carbon nanotubes and graphene, are expensive and require intricate preparation processes. Cheng *et al.* employed waste lignin recovered from black liquor for the fabrication of oxygen–nitrogen–sulfur co-doped carbon microspheres for DSSC counter electrodes *via* a straightforward process of low-temperature pre-oxidation and high-temperature self-activation.<sup>118</sup> Lignin can be utilized as a photosensitizer by complexing with DSSCs having porous nanocrystalline TiO<sub>2</sub> substrates.<sup>122</sup> Wang *et al.* developed a sustainable lignin-derived multifunctional dopant by exploiting the inherent fluorescence and self-assembly properties of lignin, and it was used in conjunction with poly(vinyl alcohol) for the fabrication of optical films with haze, fluorescence, and room-temperature phosphorescence. This dopant was also used to improve the light harvesting efficiency of solar cells. The power conversion efficiency of dye-sensitized solar cells was increased from 3.9% to 4.1% (Fig. 5B).<sup>109</sup> Currently, the application of lignin as a photoanode sensitizer in photovoltaic devices is still relatively rare and requires further research.

### 3.2. Bioimaging materials

In recent years, with the rapid development of nanotechnology and materials science, carbon quantum dots, as an emerging nanomaterial, have received widespread attention. However, most of the commonly used methods for synthesizing carbon quantum dots rely on toxic and expensive precursors, posing risks to the environment and human health. Lignin can be converted into carbon quantum dots through a series of physical and chemical methods (Fig. 6A). This synthesis method offers several advantages, including the availability of abundant raw materials, low cost and green environment. Additionally, lignin carbon quantum dots (CQDs) exhibit many superior properties that render them optimal for bioimaging applications. Pei *et al.* conducted a hydrothermal synthesis of lignin using a deionized water/nitric acid system, resulting in the conversion of lignin into CQDs for brain imaging applications. It was demonstrated that the nanoscale dimensions of lignin-derived CQDs (L-CQDs) facilitate their penetration across the blood–brain barrier, with more than 15% of living cells exhibiting internalization of L-CQDs within 1 h of incubation time.<sup>125</sup> Niu *et al.* prepared L-CQDs by molecular aggregation of cellulose lignin and demonstrated their suitability for cellular imaging under one- and two-photon excitation. These L-CQDs were found to be able to enter HeLa cells with high efficiency and to partially enter the nucleus. The fluorescence intensity of L-CQDs inside the cells increased with increasing incubation time, and the cell survival rate was found to be more than 90% even at high concentrations.<sup>126</sup> Xue *et al.* developed a lignosulfonate-based fluorescent pH sensing probe, L-SRhB, which demonstrated the ability to differentiate between normal and cancer cells. L-SRhB exhibited distinct red fluorescence in cancerous cells, whereas normal cells exhibited minimal fluorescence. L-SRhB is also pH-sensitive and can be used as a pH probe, exhibiting varying fluorescence intensity and color changes at different pH values (Fig. 6B).<sup>123</sup> Furthermore, Shi *et al.* demonstrated

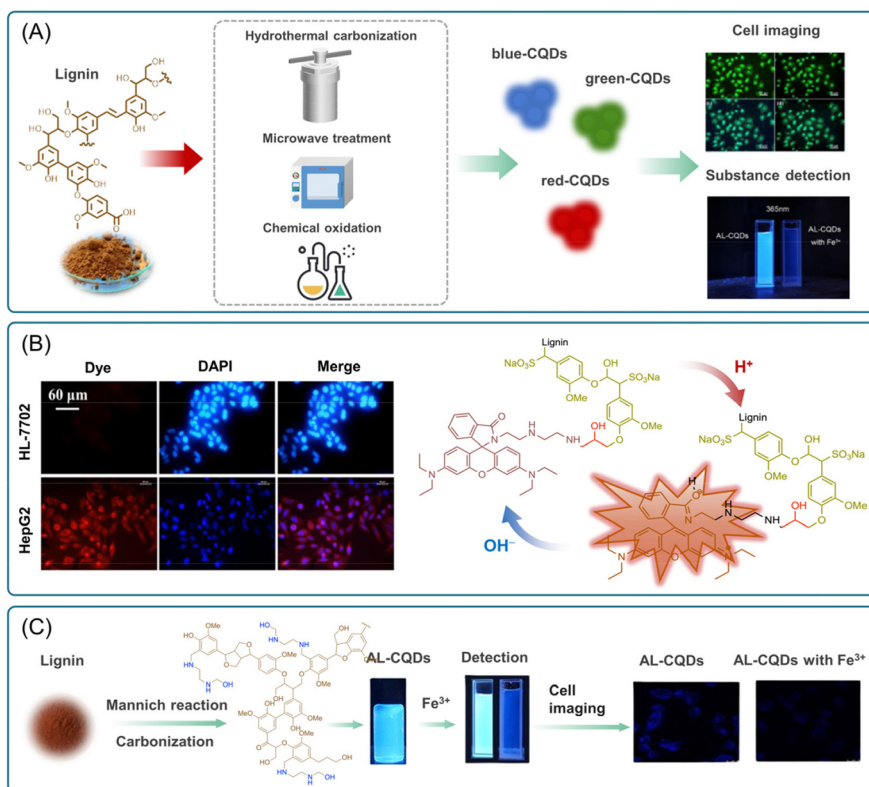


**Fig. 6** Lignin serves as a sensor and contrast agent for bioimaging. (A) Schematic diagram showing the most common approaches for the synthesis of lignin-based carbon dots for cell imaging and substance detection. (B) Fluorescence pH-sensing probe based on lignosulfonate and its application in cancer cell biomaging.<sup>123</sup> (C) Schematic diagram of AL-CQDs applied to cell imaging and intracellular ion detection.<sup>124</sup>

that AL-CQDs exhibited fluorescence quenching following the introduction of Fe<sup>3+</sup>, which was primarily attributed to electrostatic adsorption, a chelation effect, and charge transfer between AL-CQDs and Fe<sup>3+</sup> ions. These findings offer a novel approach for the detection of metal ions in biomedical and environmental monitoring applications (Fig. 6C).<sup>124</sup>

### 3.3. Transparent structural materials

Lignin, a natural polyphenolic macromolecule, provides enhanced adhesion and mechanical properties to plant cell walls. However, the dark color of industrial lignin severely limits its applications. In recent years, some researchers have identified methods for reducing the color of lignin, including chemical and physical means, which opens a new avenue for lignin in high-performance structural materials. Li *et al.* proposed a method for the removal of chromophores within the lignin, which are responsible for light absorption, while retaining the lignin structure. This innovative approach employs an alkaline H<sub>2</sub>O<sub>2</sub> treatment to selectively remove the chromophores, followed by infiltration with PMMA. The resulting transparent wood retains 80% of its lignin and achieves a light transmittance of 83% and a haze of 75%. With a thermal conductivity of 0.23 W m K<sup>-1</sup>, which is significantly lower than that of glass (1.0 W m K<sup>-1</sup>), transparent wood is an ideal material for use in buildings. This reduces the necessity for air

conditioning, lowers economic costs, and promotes energy conservation and environmental sustainability.<sup>83</sup> Another innovative method, introduced by Xia *et al.*, uses solar-assisted chemical brushing, which involves the application of hydrogen peroxide to the wood surface and subsequent removal of the lignin chromophores *via* UV light. Subsequently, epoxy resin is infiltrated into the modified wood microchannels, resulting in the formation of transparent wood with a light transmittance of over 90% and good light-guiding properties. This method allows for selective and precise bleaching, enabling the production of patterned transparent wood for various decorative and functional applications (Fig. 7A).<sup>84</sup> Shikinaka and Otsuka developed a method for whitening lignin by adjusting the solvent polarity and reacting the lignin with organic isocyanates in a water-ethanol mixture, forming nanoparticles with encapsulated chromophores. The resulting hexyl-modified lignin forms a transparent coating with 91% total light transmittance and a haze value of 7.0. Furthermore, the use of dodecyl-modified lignin allows for the formation of a transparent film at 110 °C, which can be formed after cooling between glass plates. The film can be reheated and separated for reuse (Fig. 7B).<sup>85</sup>

### 3.4. Photonic crystal materials

Photonic crystals are artificial microstructures consisting of periodic arrangements of media with different refractive

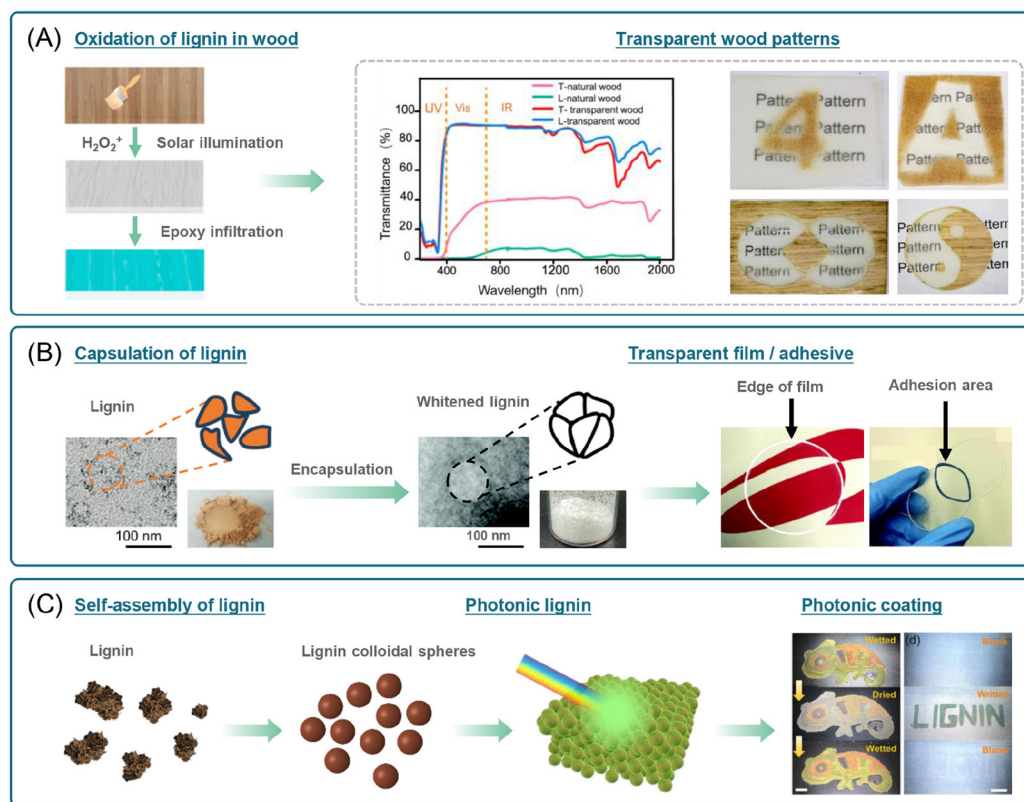


**Fig. 7** Lignin in transparent wood and photonic crystals. (A) Schematic diagram of solar-assisted fabrication of lignin-based transparent wood.<sup>84</sup> (B) Schematic of whitening a lignin-based film and advanced adhesive.<sup>85</sup> (C) Schematic representation of the preparation of photonic crystals from lignin.<sup>127</sup>

indices. They exhibit unique optical and environmental responsiveness and chemical stability, making them highly valuable in the optical, biomedical, and energy fields. In recent years, with the rapid development of lignin colloid chemistry, the method of preparing lignin colloidal particles with a uniform and tunable size has become more mature. This has led to lignin gradually becoming a promising raw material for natural polymer photonic materials. Wang and colleagues successfully utilized monodisperse lignin colloidal spheres as structural units to create short-range ordered structures, thereby achieving a critical transformation from disordered to ordered supramolecular structures in lignin. This breakthrough led to the production of lignin photonic crystals exhibiting structural color. By varying the particle size of the lignin colloidal spheres, the structural color of the lignin photonic crystals can be tuned across the entire visible spectrum. These structural colors are angle-independent and exhibit solvent responsiveness. Consequently, the researchers developed responsive structural color coatings using lignin photonic crystals, applying them in smart painting, rewritable paper, and encrypted patterns. Cytotoxicity tests demonstrated that lignin photonic crystals are compatible with human skin, blood vessels, the digestive system, and other tissue cells. This suggests their potential use in implanted/wearable optical devices, advanced cosmetics, and intelligent food packaging

(Fig. 7C).<sup>127</sup> This study has expanded the applications of lignin in advanced optical materials, providing crucial theoretical foundations and technical guidance for the development of natural polymer-based functional materials and the high-value utilization of biomass resources.

## 4. Conclusions and perspectives

In this review, we have provided a summary of the recent research in harnessing lignin for the fabrication of optical materials. Woody plants have developed and refined physical and chemical structures to harvest, convert and utilize sunlight. Remarkably, lignin provides trees with physical and (bio-)chemical resistance, as well as a broad range of optical properties, which have served as a great source of inspiration for designing synthetic micro and macroscale optical materials. The most significant advantages of lignin include not only the unique combination of optical and mechanical properties, but also important auxiliary properties, which are critical for real-world applications, such as renewability, biocompatibility, and diverse structural and interfacial chemistries. Although it is possible to synthesize molecules or materials with a specific set of optical properties, such materials often exhibit modest feedstock availability and

environmental friendliness imposing severe limitations on their sustainable scale-up industrialization and application.

As has been discussed in detail in this review, the rich chemical functionality of lignins is yet another feature that makes them more attractive as compared to inorganic materials and synthetic polymers. Although most of the currently available lignins, technical lignins, come from the pulp and biomass refining industry, where their molecular structure is disrupted to varying degrees, it is still possible by numerous physical and chemical modification methods to finely control their chemical, mechanical, and optical properties and meet the requirements set by the specific applications. Another important benefit of lignin is its good mechanical properties. By modulating the ratio and composition of rigid-flexible fragments, the strength, elasticity and flexibility of lignin-derived materials can be regulated, which is crucial for the durability of optical systems/devices for practical applications. Additionally, lignin exhibits outstanding thermal stability, which is crucial in energy harvesting applications.

Lignin, particularly technical lignin, can effectively capture solar energy and transform it into chemical energy. As previously stated in the review, the light-to-heat effect of lignin materials under sunlight conditions is approaching that of traditional inorganic carbon materials and organic photothermal materials, including carbon nanotubes, carbon spheres, polypyrrole, polyaniline, *etc.* Furthermore, the high supply of feedstock, high degree of accessibility, low cost, absence of the need for carbonization, and low energy consumption are not characteristics that can be matched by any of the aforementioned traditional photothermal materials. As a result of sustained research efforts, this abundant resource is being gradually identified as possessing a diverse range of optical properties, including UV-blocking, photoluminescence, aggregation-induced luminescence, structural color, and others. These properties have led to the identification of unique applications in energy storage, bio-imaging, intelligent buildings, anti-counterfeit coatings, and other dynamic fields, with minimal dependence on petrochemical feedstocks and minimal risk to the environment.

Despite the significant advancements that have been made in recent years, research into the optical properties of lignin is still in its infancy. The development of high-performance lignin-derived optical materials with diverse functionalities remains a fundamental challenge. Elucidation of the molecular structure of lignin is essential to fully resolve and utilize its optical properties. Nevertheless, the precise mechanisms underlying the generation of optical properties in lignin remain elusive, largely due to the paucity of precise and detailed chemical and microstructural data. Consequently, the exploration of additional optical properties of lignin is constrained, which in turn impedes the development of novel lignin-derived optical materials. Therefore, it is of the utmost importance to clarify the molecular structure of lignin and to develop molecular detection techniques in order to improve the chemical theory of lignin. This will lay the foundation for the revelation of the optical and other functional properties of lignin.

In addition, the performance stability of lignin-derived optical materials is unsatisfactory. The considerable diversity of biomass feedstocks and extraction techniques employed results in inconsistent outcomes with regard to the properties of lignin materials. This renders it challenging to draw comparisons between the findings of disparate studies. At present, the pulp and paper or biorefinery industries continue to predominantly utilise cellulose and sugar as their primary products, whereas lignin is merely separated, discarded as waste, or burned for energy. According to the characteristics of the raw materials, the quality requirements of target products and wastewater, a variety of fractionation methods, including alkaline, acidic, organic solvent, biological, and combined methods, can be employed. The application of different fractionation methods gives rise to considerable discrepancies in the structure and properties of the resulting lignin. For example, the molecular weight of lignosulfonate is typically 10 times greater than that of alkaline lignin, alkaline lignin contains a greater number of phenolic hydroxyl groups, and organosolv lignin contains a smaller number of heteroatoms. These differences directly affect the optical properties of the lignins. It is also challenging to obtain lignins with consistent properties, even when the raw material and fractionation method are the same. For example, the lignin content of poplar trees increases with age, resulting in variations in the structure and yield of lignin by-products obtained from the same alkaline fractionation method. Therefore, in order to ensure the consistent reproduction of the properties of lignin-derived optical materials in large volumes, the development of efficient, stable, and tunable fractionation techniques is essential for the standardized application of lignin materials.

Many optical materials require submicron feature sizes on the order of the wavelength of light and, in some cases, even finer control of the structure at the nanoscale. Lignin colloidal particles with high resolution (down to 20 nm) were achieved by using antisolvent, dialysis, and other micro- and nano-fabrication methods, but with very limited productivity and homogeneity. Standardized production processes and quality control are essential for the scalability and commercial viability of the applications. The precise control of the micro- and nano-scale structures of lignin-derived materials is both a necessity and a challenge. The development of efficient and stable lignin extraction and supply chain technologies is vital for improving resource utilization efficiency and ensuring the consistent supply and quality of lignin materials, particularly in industrial production where cost and performance are equally important.

In conclusion, the exploitation of the distinctive optical properties of lignin opens up a new avenue for lignin valorization. The precise and demand-driven regulation of lignin molecular, micro- and macro-structures, so that it exhibits unique optical properties such as ultraviolet absorption, phosphorescence, fluorescence, and photothermal conversion, can result in the generation of a diverse range of novel functional materials. With in-depth studies in chemistry, biology, physics, and materials, lignin, an ancient natural polymer, will continue to

be the abundant natural resource for new materials, showing more possibilities.

## Author contributions

Hai Liu: methodology, visualization, writing – original draft. Yanhua Guan: review and editing. Li Yan: review and editing. Yong Zheng: review and editing. Chuanling Si: review and editing. Lin Dai: supervision, conceptualization, visualization, writing, review and editing, funding acquisition.

## Data availability

No primary research results, software or code have been included and no new data were generated or analysed as part of this review.

## Conflicts of interest

The authors declare that they have no known competing financial interests or personal relationships that could have appeared to influence the work reported in this paper.

## Acknowledgements

This work was supported by the National Natural Science Foundation of China (32171717, 32271814), the Natural Science Foundation of Tianjin (22JCYBJC01560, 23JCZDJC00630), and the China Postdoctoral Science Foundation (2023M740562).

## References

- 1 B. L. Tardy, E. Lizundia, C. Guizani, M. Hakkarainen and M. H. Sipponen, *Mater. Today*, 2023, **65**, 122–132.
- 2 C. A. Torres, C. Azocar, P. Ramos, R. Pérez-Díaz, G. Sepulveda and M. A. Moya-León, *Hortic. Res.*, 2020, **7**, 22.
- 3 M. Gigli and C. Crestini, *Green Chem.*, 2020, **22**, 4722–4746.
- 4 Y. Qian, Y. Deng, H. Li and X.-q. Qiu, *Ind. Eng. Chem. Res.*, 2014, **53**, 10024–10028.
- 5 H. Zhang, S. Fu and Y. Chen, *Int. J. Biol. Macromol.*, 2020, **147**, 607–615.
- 6 Y. Li, S. Zhao, Y. Li, A. J. Ragauskas, X. Song and K. Li, *Int. J. Biol. Macromol.*, 2022, **223**, 1287–1296.
- 7 H. Zhang, X. Liu, S. Fu and Y. Chen, *Int. J. Biol. Macromol.*, 2019, **133**, 86–92.
- 8 N. Luo, M. Wang, H. Li, J. Zhang, T. Hou, H. Chen, X. Zhang, J. Lu and F. Wang, *ACS Catal.*, 2017, **7**, 4571–4580.
- 9 X. Cheng, B. Palma, H. Zhao, H. Zhang, J. Wang, Z. Chen and J. Hu, *ChemSusChem*, 2023, **16**, e202300675.
- 10 A. J. Stamm, J. Semb and E. E. Harris, *J. Phys. Chem.*, 1931, **36**, 1574–1584.
- 11 M. Takada, Y. Okazaki, H. Kawamoto and T. Sagawa, *ACS Omega*, 2022, **7**, 5096–5103.
- 12 B. Albinsson, S. Li, K. Lundquist and R. Stomberg, *J. Mol. Struct.*, 1999, **508**, 19–27.
- 13 Y. Xue, X. Qiu, Y. Wu, Y. Qian, M. Zhou, Y. Deng and Y. Li, *Polym. Chem.*, 2016, **7**, 3502–3508.
- 14 J. Xu, C. Li, L. Dai, C. Xu, Y. Zhong, F. Yu and C. Si, *ChemSusChem*, 2020, **13**, 4284–4295.
- 15 S. Barsberg, T. Elder and C. Felby, *Chem. Mater.*, 2003, **15**, 649–655.
- 16 A. N. Cauley and J. N. Wilson, *Biomater. Sci.*, 2017, **5**, 2114–2121.
- 17 Y. Jiang, Z. Wang, L. Zhou, S. Jiang, X. Liu, H. Zhao, Q. Huang, L. Wang, G. Chen and S. Wang, *Int. J. Biol. Macromol.*, 2022, **206**, 264–276.
- 18 Y. Xue, X. Qiu, Z. Liu and Y. Li, *ACS Sustainable Chem. Eng.*, 2018, **6**, 7695–7703.
- 19 Y. Zheng, A. Moreno, Y. Zhang, M. H. Sipponen and L. Dai, *Trends Chem.*, 2024, **6**, 62–78.
- 20 Y. Zheng, H. Liu, L. Yan, H. Y. Yang, L. Dai and C. L. Si, *Adv. Funct. Mater.*, 2024, **34**, 2310653.
- 21 Y. Yang, Y. Guan, C. Li, T. Xu, L. Dai, J. Xu and C. Si, *Adv. Compos. Hybrid Mater.*, 2024, **7**, 61.
- 22 H. Zhou, Y. R. Mao, Y. Zheng, T. T. Liu, Y. F. Yang, C. L. Si, L. Wang and L. Dai, *Chem. Eng. J.*, 2023, **471**, 144572.
- 23 Y. Zheng, T. Liu, H. He, Z. Lv, J. Xu, D. Ding, L. Dai, Z. Huang and C. Si, *Adv. Compos. Hybrid Mater.*, 2023, **6**, 53.
- 24 J. Xu, R. Liu, L. Wang, A. Pranovich, J. Hemming, L. Dai, C. Xu and C. Si, *Adv. Compos. Hybrid Mater.*, 2023, **6**, 214.
- 25 W. Li, H. Sun, G. Wang, W. Sui, L. Dai and C. Si, *Green Chem.*, 2023, **25**, 2241–2261.
- 26 Q. W. Cao, Q. Wu, L. Dai, X. J. Shen and C. L. Si, *Green Chem.*, 2021, **23**, 2329–2335.
- 27 M. Ma, L. Dai, J. Xu, Z. Liu and Y. Ni, *Green Chem.*, 2020, **22**, 2011–2017.
- 28 L. Dai, M. S. Ma, J. K. Xu, C. L. Si, X. H. Wang, Z. Liu and Y. H. Ni, *Chem. Mater.*, 2020, **32**, 4324–4330.
- 29 S. Constant, H. L. J. Wienk, A. E. Frissen, P. d. Peinder, R. Boelens, D. S. van Es, R. J. H. Grisel, B. M. Weckhuysen, W. J. J. Huijgen, R. J. A. Gosselink and P. C. A. Bruijninx, *Green Chem.*, 2016, **18**, 2651–2665.
- 30 J. Lei, L. Chen, J. Lin, W. Liu, Q. Xiong and X. Qiu, *Green Chem.*, 2024, **26**, 2143–2156.
- 31 K. Lundquist, B. Josefsson and G. Nyquist, *Holzforschung*, 1978, **32**, 27–32.
- 32 I. V. Pylypchuk, P. A. Lindén, M. E. Lindström and O. Sevastyanova, *ACS Sustainable Chem. Eng.*, 2020, **8**, 13805–13812.
- 33 H. D. Thi, K. Van Aelst, S. Van den Bosch, R. Katahira, G. T. Beckham, B. F. Sels and K. M. Van Geem, *Green Chem.*, 2022, **24**, 191–206.

- 34 A. D. Bruhn, U. Wünsch, C. L. Osburn, J. C. Rudolph and C. A. Stedmon, *Limnol. Oceanogr.: Methods*, 2023, **21**, 508–528.
- 35 C. M. L. de Melo, I. J. da Cruz Filho, G. F. de Sousa, G. A. de Souza Silva, D. K. D. do Nascimento Santos, R. S. da Silva, B. R. de Sousa, R. G. de Lima Neto, M. do Carmo Alves de Lima and G. J. de Moraes Rocha, *Int. J. Biol. Macromol.*, 2020, **162**, 1725–1733.
- 36 C. S. Lancefield, S. Constant, P. de Peinder and P. C. A. Bruijninx, *ChemSusChem*, 2019, **12**, 1139–1146.
- 37 X. Zhang, *RSC Adv.*, 2021, **11**, 13124–13129.
- 38 Y. Zhang, L. Yang, D. Wang and D. Li, *Int. J. Biol. Macromol.*, 2018, **107**, 1193–1202.
- 39 F. Xiong, L. Zhou, L. Qian and S. Liu, *BioResources*, 2014, **10**, 1149–1161.
- 40 Y. Qian, X. Qiu and S. Zhu, *ACS Sustainable Chem. Eng.*, 2016, **4**, 4029–4035.
- 41 V. K. Thakur, M. K. Thakur, P. Raghavan and M. R. Kessler, *ACS Sustainable Chem. Eng.*, 2014, **2**, 1072–1092.
- 42 Y. Qian, X. Qiu and S. Zhu, *Green Chem.*, 2015, **17**, 320–324.
- 43 H. Sadeghifar, R. A. Venditti, J. S. Jur, R. E. Gorga and J. J. Pawlak, *ACS Sustainable Chem. Eng.*, 2017, **5**, 625–631.
- 44 M. Parit, P. Saha, V. A. Davis and Z. Jiang, *ACS Omega*, 2018, **3**, 10679–10691.
- 45 M. H. Tran, D.-P. Phan and E. Y. Lee, *Green Chem.*, 2021, **23**, 4633–4646.
- 46 N. Ratanasumarn and P. Chitprasert, *Int. J. Biol. Macromol.*, 2020, **153**, 138–145.
- 47 M. Jablonský, A. Ház and J. Šima, *Cellul. Chem. Technol.*, 2015, **49**, 267–274.
- 48 T. G. M. Smijs and S. Pavel, *Nanotechnol., Sci. Appl.*, 2011, **4**, 95–112.
- 49 Y. Zhang and M. Naebe, *ACS Sustainable Chem. Eng.*, 2021, **9**, 1427–1442.
- 50 R. Kaur, N. S. Thakur, S. Chandna and J. Bhaumik, *ACS Sustainable Chem. Eng.*, 2021, **9**, 11223–11237.
- 51 H. Wang, W. Lin, X. Qiu, F. Fu, R. Zhong, W. Liu and D. Yang, *ACS Sustainable Chem. Eng.*, 2018, **6**, 3696–3705.
- 52 C. Shi, S. Zhang, W. Wang, R. J. Linhardt and A. J. Ragauskas, *ACS Sustainable Chem. Eng.*, 2020, **8**, 22–28.
- 53 Y. Yang, R. Zhao, T. Zhang, K. Zhao, P. Xiao, Y. Ma, P. M. Ajayan, G. Shi and Y. Chen, *ACS Nano*, 2018, **12**, 829–835.
- 54 K.-K. Liu, Q. Jiang, S. Tadepalli, R. Raliya, P. Biswas, R. R. Naik and S. Singamaneni, *ACS Appl. Mater. Interfaces*, 2017, **9**, 7675–7681.
- 55 C. Chen, C. Chen, Y. Li, J. Song, Z. Yang, Y. Kuang, E. Hitz, C. Jia, A. Gong, F. Jiang, J. Zhu, B. Yang, J. Xie and L. Hu, *Adv. Mater.*, 2017, **29**, 1701756.
- 56 X. Yang, Y. Yang, L. Fu, M. Zou, Z. Li, A. Cao and Q. Yuan, *Adv. Funct. Mater.*, 2018, **28**, 1704505.
- 57 Q. Hou, C. Xue, N. Li, H. Wang, Q. Chang, H. Liu, J. Yang and S. Hu, *Carbon*, 2019, **149**, 556–563.
- 58 D. Zhao and T. Chung, *Water Res.*, 2018, **147**, 43–49.
- 59 G. Liua, J. Xub and K. Wangc, *Nano Energy*, 2017, **41**, 269–284.
- 60 J. Lei, L. Chen, J. Lin, W. Liu, Q. Xiong and X. Qiu, *Green Chem.*, 2024, **26**, 2143–2156.
- 61 M. Lang, F. Stober and H. K. Lichtenthaler, *Radiat. Environ. Biophys.*, 1991, **30**, 333–347.
- 62 A. Castellan, H. Choudhury, R. S. Davidson and S. Grelier, *J. Photochem. Photobiol., A*, 1994, **81**, 117–122.
- 63 H. Tylli, I. Forsskåhl and C. Olkkonen, *J. Photochem. Photobiol., A*, 1995, **87**, 181–191.
- 64 C. Gardrat, R. Ruggiero, W. Hoareau, A. Nourmamode, S. Grelier, B. Siegmund and A. Castellan, *J. Photochem. Photobiol., A*, 2004, **167**, 111–120.
- 65 A. Lähdetie, P. Nousiainen, J. Sipilä, T. Tamminen and A.-S. Jääskeläinen, *Holzforschung*, 2013, **67**, 531–538.
- 66 K. Radotić, A. Kalauzi, D. Djikanović, M. Jeremić, R. M. Leblanc and Z. G. Cerović, *J. Photochem. Photobiol., B*, 2006, **83**, 1–10.
- 67 Y. Xue, X. Qiu and X. Ouyang, *Int. J. Biol. Macromol.*, 2020, **154**, 981–988.
- 68 H. Zhang, Y. Bai, W. Zhou and F. Chen, *Int. J. Biol. Macromol.*, 2017, **97**, 201–208.
- 69 J. Liu, M. Nero, K. Jansson, T. Willhammar and M. Sipponen, *Nat. Commun.*, 2023, **14**, 3099.
- 70 Z. Tu, J. Wang, W. Liu, Z. Chen, J. Huang, J. Li, H. Lou and X. Qiu, *Mater. Horiz.*, 2022, **9**, 2613–2625.
- 71 J. Li, W. Liu, X. Qiu, X. Zhao, Z. Chen, M. Yan, Z. Fang, Z. Li, Z. Tu and J. Huang, *Green Chem.*, 2022, **24**, 823–836.
- 72 X. Zhao, C. Huang, D. Xiao, P. Wang, X. Luo, W. Liu, S. Liu, J. Li, S. Li and Z. Chen, *ACS Appl. Mater. Interfaces*, 2021, **13**, 7600–7607.
- 73 Q. Shao, Y. Luo, M. Cao, X. Qiu and D. Zheng, *Chem. Eng. J.*, 2023, **476**, 146678.
- 74 X. Zhao, L. Shi, B. Tian, S. Li, S. Liu, J. Li, S. Liu, T. D. James and Z. Chen, *J. Mater. Chem. A*, 2023, **11**, 12308–12314.
- 75 J. Mei, N. L. C. Leung, R. T. K. Kwok, J. W. Y. Lam and B. Z. Tang, *Chem. Rev.*, 2015, **115**, 11718–11940.
- 76 H. Wang, E. Zhao, J. W. Y. Lam and B. Z. Tang, *Mater. Today*, 2015, **18**, 365–377.
- 77 S.-Y. Yang, Y. Chen, R. K. Kwok, J. Lam and B. Tang, *Chem. Soc. Rev.*, 2024, **53**, 5366–5393.
- 78 M. Yan, D. Yang, Y. Deng, P. Chen, H. Zhou and X.-q. Qiu, *Colloids Surf., A*, 2010, **371**, 50–58.
- 79 Y. Deng, X. Feng, M. Zhou, Y. Qian, H. Yu and X.-q. Qiu, *Biomacromolecules*, 2011, **124**, 1116–1125.
- 80 Y. Deng, X. Feng, D. Yang, C. Y. Yi and X.-q. Qiu, *BioResources*, 2012, **7**, 1145–1156.
- 81 Z. Ma, C. Liu, N. Niu, Z. Chen, S. Li, S. Liu and J. Li, *ACS Sustainable Chem. Eng.*, 2018, **6**, 3169–3175.
- 82 J. Wang, Y. Deng, Y. Qian, X. Qiu, Y. Ren and D. Yang, *Green Chem.*, 2016, **18**, 695–699.
- 83 Y. Li, Q. Fu, R. Rojas, M. Yan, M. Lawoko and L. Berglund, *ChemSusChem*, 2017, **10**, 3445–3451.

- 84 Q. Xia, C. Chen, T. Li, S. He, J. Gao, X. Wang and L. Hu, *Sci. Adv.*, 2021, 7, eabd7342.
- 85 K. Shikinaka and Y. Otsuka, *Green Chem.*, 2022, 24, 3243–3249.
- 86 H. Yin, B. Dong, X. Liu, T.-M. Zhan, L. Shi, J. Zi and E. Yablonovitch, *Proc. Natl. Acad. Sci. U. S. A.*, 2012, 109, 10798–10801.
- 87 D. G. Stavenga, H. L. Leertouwer, D. C. Osorio and B. D. Wilts, *Light: Sci. Appl.*, 2015, 4, e243–e243.
- 88 J. Wang, W. Chen, D. Yang, Z. Fang, W. Liu, T. Xiang and X.-q. Qiu, *Small*, 2022, e2200671.
- 89 X. Jin, X. Liu, X. Li, L. Du, L. Su, Y. Ma and S. Ren, *Int. J. Biol. Macromol.*, 2022, 219, 44–52.
- 90 S. Jiang, Z. Zhang, T. Zhou, S. Duan, Z. Yang, Y. Ju, C. Jia, X. Lu and F. Chen, *Desalination*, 2022, 531, 115706.
- 91 T. Yang, H. Zhang, C. Huang, C. Cai, C. Gerhard and K. Zhang, *Small Methods*, 2023, 7, 2300913.
- 92 J. Gu and K. Ruan, *Nano-Micro Lett.*, 2021, 13, 110.
- 93 H. Zhou, L. Yan, D. Tang, T. Xu, L. Dai, C. Li, W. Chen and C. Si, *Adv. Mater.*, 2024, 33, 2403876.
- 94 Y. Yang, H. Zhou, X. Chen, T. Liu, Y. Zheng, L. Dai and C. Si, *Chem. Eng. J.*, 2023, 477, 147216.
- 95 P. Tao, G. Ni, C. Song, W. Shang, J. Wu, J. Zhu, G. Chen and T. Deng, *Nat. Energy*, 2018, 3, 1031–1041.
- 96 W. Shang and T. Deng, *Nat. Energy*, 2016, 1, 16133.
- 97 H. Liu, Z. Huang, K. Liu, X. Hu and J. Zhou, *Adv. Energy Mater.*, 2019, 9, 1900310.
- 98 J. Jeon, S. H. Lee, S.-R. Lee, T. H. Seo and Y.-K. Kim, *ACS Appl. Mater. Interfaces*, 2023, 15, 30692–30706.
- 99 S. Chen, L. Sun, Y. Huang, D. Yang, M. Zhou and D. Zheng, *Carbon Neutralization*, 2023, 2, 494–509.
- 100 X. Lin, P. Wang, R. Hong, X. Zhu, Y. Liu, X. Pan, X. Qiu and Y. Qin, *Adv. Funct. Mater.*, 2022, 32, 2209262.
- 101 Y. Gu, D. Wang, Y. Gao, Y. Yue, W. Yang, C. Mei, X. Xu, Y. Xu, H. Xiao and J. Han, *Adv. Funct. Mater.*, 2023, 33, 2306947.
- 102 Y. Wu, J. Wang, X. Qiu, R. Yang, H. Lou, X. Bao and Y. Li, *ACS Appl. Mater. Interfaces*, 2016, 8, 12377–12383.
- 103 T. Li, H. Liu, X. Zhao, G. Chen, J. Dai, G. Pastel, C. Jia, C. Chen, E. Hitz, D. Siddhartha, R. Yang and L. Hu, *Adv. Funct. Mater.*, 2018, 28, 1707134.
- 104 X. Wu, G. Y. Chen, W. Zhang, X. Liu and H. Xu, *Adv. Sustainable Syst.*, 2017, 1, 1700046.
- 105 Y. Li and N. Hong, *J. Mater. Chem. A*, 2015, 3, 21537–21544.
- 106 Y. Xi, S. Huang, D. Yang, X. Qiu, H. Su, C. Yi and Q. Li, *Green Chem.*, 2020, 22, 4321–4330.
- 107 G. A. Al-Dainy, F. Watanabe, G. K. Kannarpady, A. Ghosh, B. Berry, A. S. Biris and S. E. Bourdo, *ACS Omega*, 2020, 5, 1887–1901.
- 108 Y. Li, T. Liu, X. Qiu, Y. Zhou and Y. Li, *ACS Sustainable Chem. Eng.*, 2019, 7, 961–968.
- 109 X. Wang, H. Guo, Z. Lu, X. Liu, X. Luo, S. Li, S. Liu, J. Li, Y. Wu and Z. Chen, *ACS Appl. Mater. Interfaces*, 2021, 13, 33536–33545.
- 110 H.-C. Hu, H. Xu, J. Wu, L. Li, F. Yue, L. Huang, L. Chen, X. Zhang and X. Ouyang, *Adv. Funct. Mater.*, 2020, 30, 2001494.
- 111 M. Fahlman, S. Fabiano, V. Gueskine, D. Simon, M. Berggren and X. Crispin, *Nat. Rev. Mater.*, 2019, 4, 627–650.
- 112 J.-K. Tan, R.-Q. Png, C. Zhao and P. K. H. Ho, *Nat. Commun.*, 2018, 9, 3269.
- 113 Y. Zhou, C. Fuentes-Hernandez, J. Shim, J. Meyer, A. J. Giordano, H. Li, P. Winget, T. Papadopoulos, H. Cheun, J. Kim, M. Fenoll, A. Dindar, W. Haske, E. Najafabadi, T. M. Khan, H. Sojoudi, S. Barlow, S. Graham, J.-L. Brédas, S. R. Marder, A. Kahn and B. Kippelen, *Science*, 2012, 336, 327–332.
- 114 S. Xiong, L. Hu, L. Hu, L. Sun, F. Qin, X. Liu, M. Fahlman and Y. Zhou, *Adv. Mater.*, 2019, 31, 1806616.
- 115 M. Du, X. Zhu, L. Wang, H. Wang, J. Feng, X. Jiang, Y. Cao, Y. Sun, L. Duan, Y. Jiao, K. Wang, X. Ren, Z. Yan, S. Pang and S. Liu, *Adv. Mater.*, 2020, 32, 2004979.
- 116 Q. Kang, Q. Wang, C. An, C. He, B. Xu and J. Hou, *J. Energy Chem.*, 2020, 43, 40–46.
- 117 Q. Zhang, T. Liu, S. Wilken, S. Xiong, H. Zhang, I. Ribca, M. Liao, X. Liu, R. Kroon, S. Fabiano, F. Gao, M. Lawoko, Q. Bao, R. Österbacka, M. Johansson and M. Fahlman, *Adv. Mater.*, 2024, 36, 2307646.
- 118 W. Cheng, C. Wan, X. Li, H. Chai, Z. Yang, S. Wei, J. Su, X. Tang and Y. Wu, *J. Energy Chem.*, 2023, 83, 549–563.
- 119 P. Schlee, S. Hérou, R. Jervis, P. Shearing, D. Brett, D. Baker, O. Hosseinaei, P. Tomani, M. M. Murshed, Y. Li, M. J. Mostazo-López, D. Cazorla-Amorós, A. J. J. Sobrido and M. Titirici, *Chem. Sci.*, 2019, 10, 2980–2988.
- 120 P. Schlee, O. Hosseinaei, D. Baker, A. Landmér, P. Tomani, M. J. Mostazo-López, D. Cazorla-Amorós, S. Hérou and M. Titirici, *Carbon*, 2019, 145, 470–480.
- 121 A. Beaucamp, M. Muddasar, I. S. Amiinu, M. M. Leite, M. Culebras, K. Latha, M. Gutiérrez, D. Rodríguez-Padrón, F. d. Monte, T. Kennedy, K. Ryan, R. Luque, M. Titirici and M. Collins, *Green Chem.*, 2022, 24, 8193–8226.
- 122 M. M. Hasan, M. D. Islam and T. U. Rashid, *Energy Fuels*, 2020, 34, 15634–15671.
- 123 Y. Xue, W. Liang, Y. Li, Y. Wu, X. Peng, X. Qiu, J. Liu and R. Sun, *J. Agric. Food Chem.*, 2016, 64, 9592–9600.
- 124 Y. Shi, X. Liu, M. Wang, J. Huang, X. Jiang, J. Pang, F. Xu and X. Zhang, *Int. J. Biol. Macromol.*, 2019, 128, 537–545.
- 125 Y. Pei, A. Y. Chang, X. Liu, H. Wang, H. Zhang, A. Radadia, Y. Wang, W. W. Yu and S. Wang, *AIChE J.*, 2021, 67, e17132.
- 126 N. Niu, Z. Ma, F. He, S. Li, J. Li, S. Liu and P. Yang, *Langmuir*, 2017, 33, 5786–5795.
- 127 J. Wang, W. Chen, D. Yang, Z. Fang, W. Liu, T. Xiang and X. Qiu, *ACS Nano*, 2022, 16, 20705–20713.